



# Learning where to look for COVID-19 growth: Multivariate analysis of COVID-19 cases over time using explainable convolution–LSTM



Novanto Yudistira <sup>a,\*</sup>, Sutiman Bambang Sumitro <sup>b</sup>, Alberth Nahas <sup>c,d</sup>, Nelly Florida Riama <sup>d</sup>

<sup>a</sup> Faculty of Computer Science, University of Brawijaya, Indonesia

<sup>b</sup> Faculty of Mathematics and Natural Science, University of Brawijaya, Indonesia

<sup>c</sup> Department of Marine, Earth, and Atmospheric Sciences, North Carolina State University Raleigh, United States of America

<sup>d</sup> Indonesian Agency for Meteorology, Climatology and Geophysics, Center for Research and Development, Indonesia

## ARTICLE INFO

### Article history:

Received 21 February 2021

Received in revised form 20 April 2021

Accepted 28 April 2021

Available online 7 May 2021

### Keywords:

COVID-19

Multivariate

Visual explanation

LSTM prediction

## ABSTRACT

Determinant factors which contribute to the prediction should take into account multivariate analysis for capturing coarse-to-fine contextual information. From the preliminary descriptive analysis, it shows that environmental factor such as UV (ultraviolet) is one of the essential factors that should be considered to observe the COVID-19 epidemic drivers. Moreover, there are education, government, morphological, health, economic, and behavioral factors contributing to the growth of COVID-19. Besides descriptive analysis, in this research, multivariate analysis is considered to provide comprehensive explanations about factors contributing to pandemic dynamics. To achieve rich explanations, visual attribution of explainable Convolution-LSTM is utilized to see high contributing factors responsible for the growth of daily COVID-19 cases. Our model consists of 1 D CNN in the first layer to capture local relationships among variables followed by LSTM layers to capture local dependencies over time. It produces the lowest prediction errors compared to the other existing models. This permits us to employ gradient-based visual attribution for generating saliency maps for each time dimension and variable. These are then used for explaining which variables throughout which period of the interval is contributing for a given time-series prediction, likewise as explaining that during that time intervals were the joint contribution of most vital variables for that prediction. The explanations are useful for stakeholders to make decisions during and post pandemics. The explainable Convolution-LSTM code is available here: <https://github.com/cbasemaster/time-series-attribution>.

© 2021 Elsevier B.V. All rights reserved.

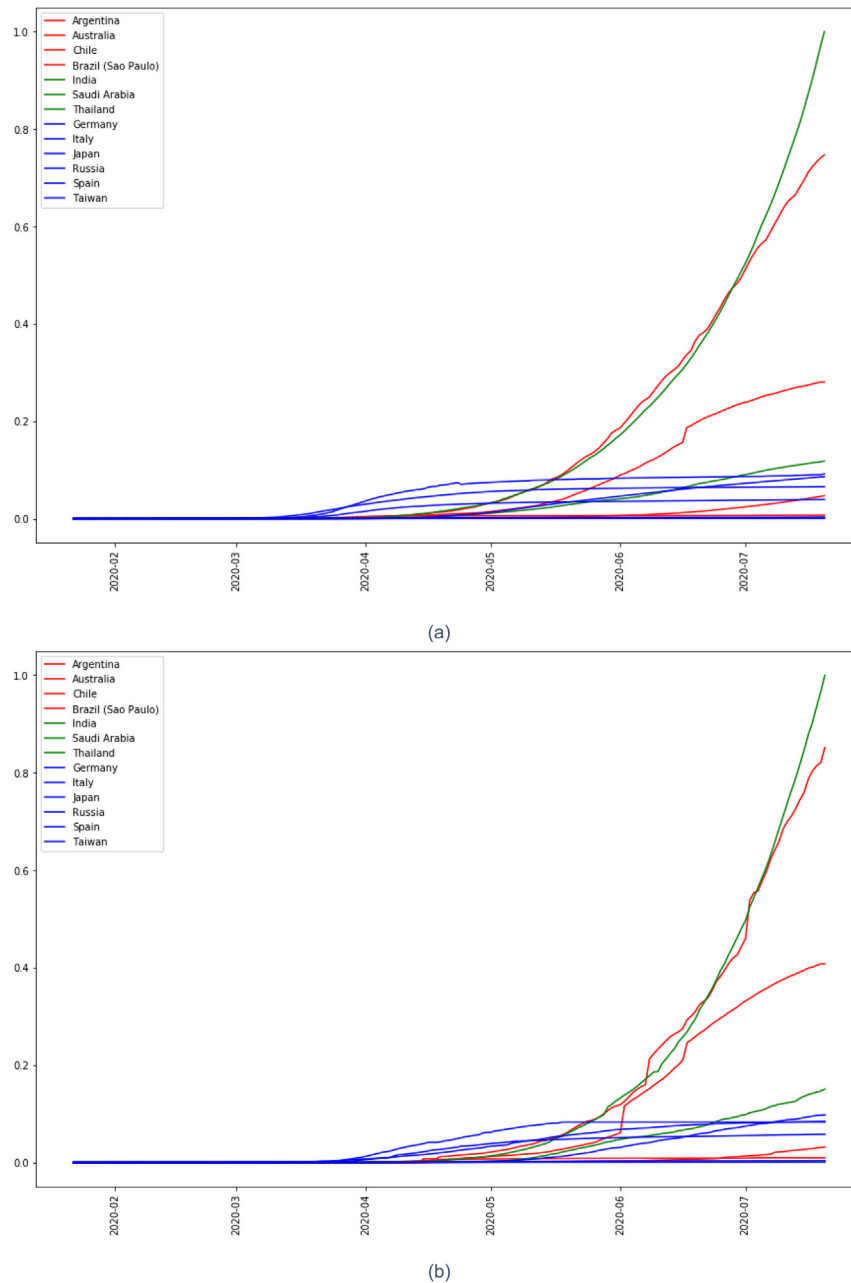
## 1. Introduction

The Wuhan Municipal Health Commission first detected the 2019 Coronavirus Disease (COVID-19) in Hubei Province, China, and early information about the outbreak has been sent to the World Health Organization (WHO) [1,2]. As the number of people exposed to COVID-19 increases, the disease's ability to spread in the community has rapidly improved. The rapid growth involves evidence of person-to-person transmission, indicating that COVID-19 is highly contagious. COVID-19 can also live actively in the air and on the ground [3,4]. Environmental factors are affecting the success of airborne viruses spreading among susceptible hosts [5]. These forms of transmission may cause a pandemic. A pandemic can cause severe activity and death in a wide geographic area [6]. To withstand the spread of COVID-19, a natural factor that is rarely discussed is ultraviolet (UV). Many UV papers prove that it can inactivate viruses [7,8], especially

ultraviolet rays from sunlight [9]. An example of virus inactivation by ultraviolet light is ultraviolet-C radiation for virus inactivation [8]. Even though ultraviolet rays can inactivate the virus, it will not be evident if the pollution level is high [10]. Please note that smoke particles will weaken ultraviolet light's ability to exist in the air [11]. Efforts to reduce the spread of COVID-19 can also reduce carbon emissions by reducing the intensity of travel worldwide [12], which is good for the environment. Moreover, vaccine development is not sufficient, and it takes a long time to discover [13]. Therefore, urgent, large-scale, and natural immunity is needed. Some technologies have been developed by using UV light [14,15]. Based on the above evidences, we investigate how UV rays dynamically affect the spread of COVID-19 based on geographic location, pollution levels, and human activities. The fast-growing of digital health enables us to gather health data massively from sensors attached to patients [16]. Consequently, data considered in this research like cardiovascular death rates, diabetes prevalence, and the number of hospital beds per thousand are now possible to be collected in quantity over time. Multivariate time-series data analysis is a better choice

\* Corresponding author.

E-mail address: [yudistira@ub.ac.id](mailto:yudistira@ub.ac.id) (N. Yudistira).

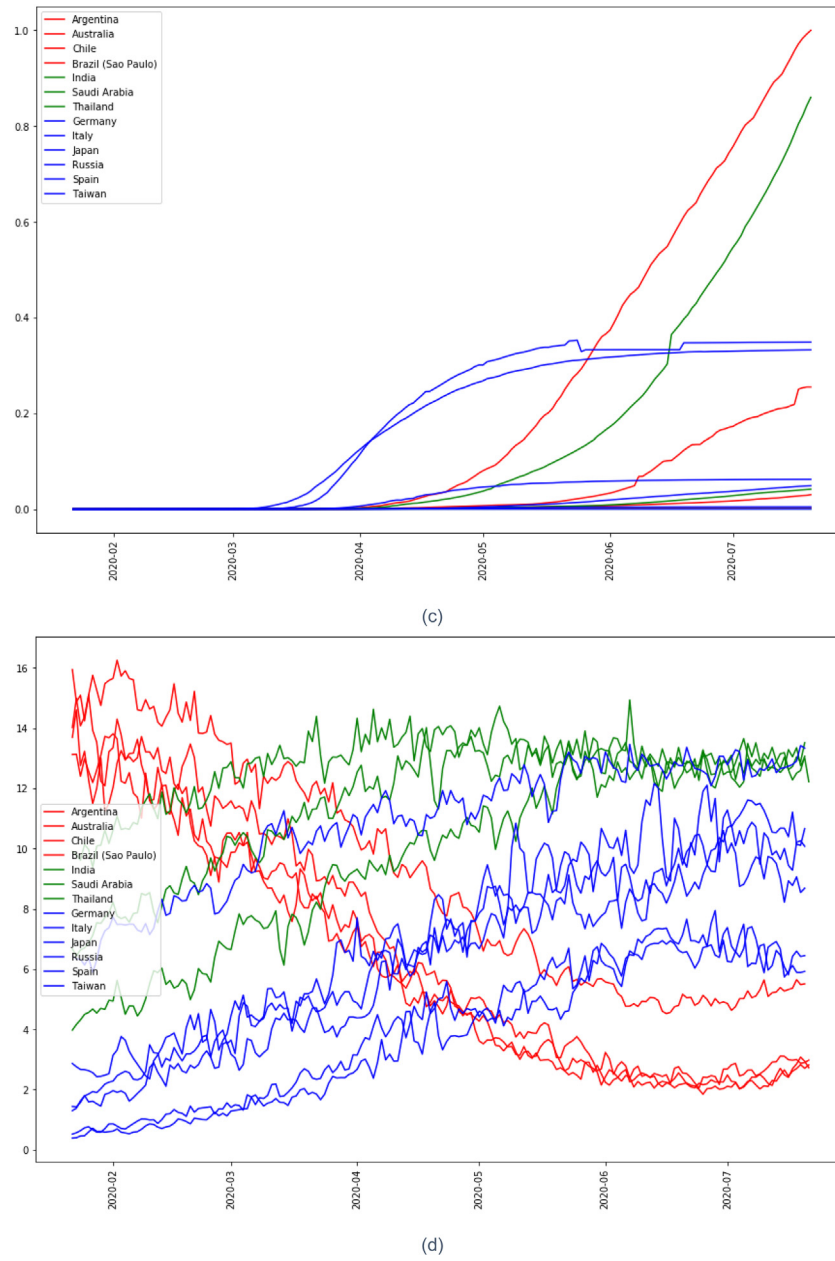


**Fig. 1.** (a) The growth of cumulative confirmed cases in northern subtropical (blue), tropical (green), and southern subtropical (red) countries (b) The growth of cumulative recovered cases in northern subtropical (blue), tropical (green), and southern subtropical (red) countries (c) The growth of cumulative death cases in northern subtropical (blue), tropical (green), and southern subtropical (red) countries (d) Daily mean UV Index dynamics over time of northern subtropical (blue), tropical (green) and southern subtropical (red).

for analyzing the growth of the COVID-19 pandemic because it has interdependence among multiple factors over time. The classification of multivariate time-series is also an emerging hot topic in machine learning [17].

The transmission dynamics were investigated by [18] consisting of susceptible, exposed, infected, and recovered individuals using differential equations. It shows explanations in form of correlation of its parameter to prediction. However, it only considers variables without time-series information of which differs from us. Time-series information is problematic especially at the beginning of a pandemic where the direction of dynamics is still unknown. In that case, early forecasting is desirable even though the availability of data is small. Polynomial Neural Network (PNN) with corrective feedback was proposed to reduce uncertainty and increase the robustness of the model trained on

a small dataset [19]. Deep neural network (DNN) can capture information from big data, thus it is the best candidate to perform classification tasks [20,21]. The ability of DNN to generate meaningful feature representations in the learning process has attracted attention in the machine learning and data science circles. In this study, we use interpretable DNN forecasts to perform multivariate time series data analysis. This explanation helps to find critical joint characteristics to predict daily cases of COVID-19 over a period of time. One study using interpretable DNN is Roy Assaf et al.'s multivariate multi-factory PV energy prediction, [22] which uses a two-stage convolutional neural network (CNN). The explanation provided by DNN is beneficial for policymakers to formalize the framework to be implemented during and post-pandemic such as in tourism [23].

**Fig. 1. (continued).**

Based on the aforementioned evidences and problems, our works have 4 contributions:

1. We provide descriptive and statistical analysis of the relationship of environmental and mobility factors in regards to the dynamics of COVID-19.
2. We proposed a model that able to predict the COVID-19 pandemic over time consisting of 1D CNN with  $1 \times 1$  kernels each of which has 59 channels followed by LSTM layers to capture a multivariate time-series pattern.
3. We proposed gradient-based visual attribution for generating a saliency map to explain which variables during which period contributing to daily new cases.
4. Explaining important factors contributing to the dynamics of COVID-19 pandemics for understanding the current situation about why the number of new cases appears to increase.

The remainder of this paper is organized as follows. Section 2 describes material and methods which explains variables considered in this research. Section 3 explains the setup applied throughout experiments and data sets applied in this research. Section 4 shows the results of reconstruction and discusses explanations produced by the network, and the last section concludes the research.

## 2. Materials and methods

### 2.1. Multidimensional factors

**Table 1** shows 59 factors used in this COVID-19 growth multivariate time-series analysis ranging from environmental, social, government, economical to behavioral factors. The clear-sky UV index (UVIEF) is a measure for the effective UV irradiance (1 unit equals  $25 \text{ mW/m}^2$ ) reaching the Earth's surface. The UV dose is the effective UV irradiance (given in  $\text{kJ/m}^2$ ), reaching

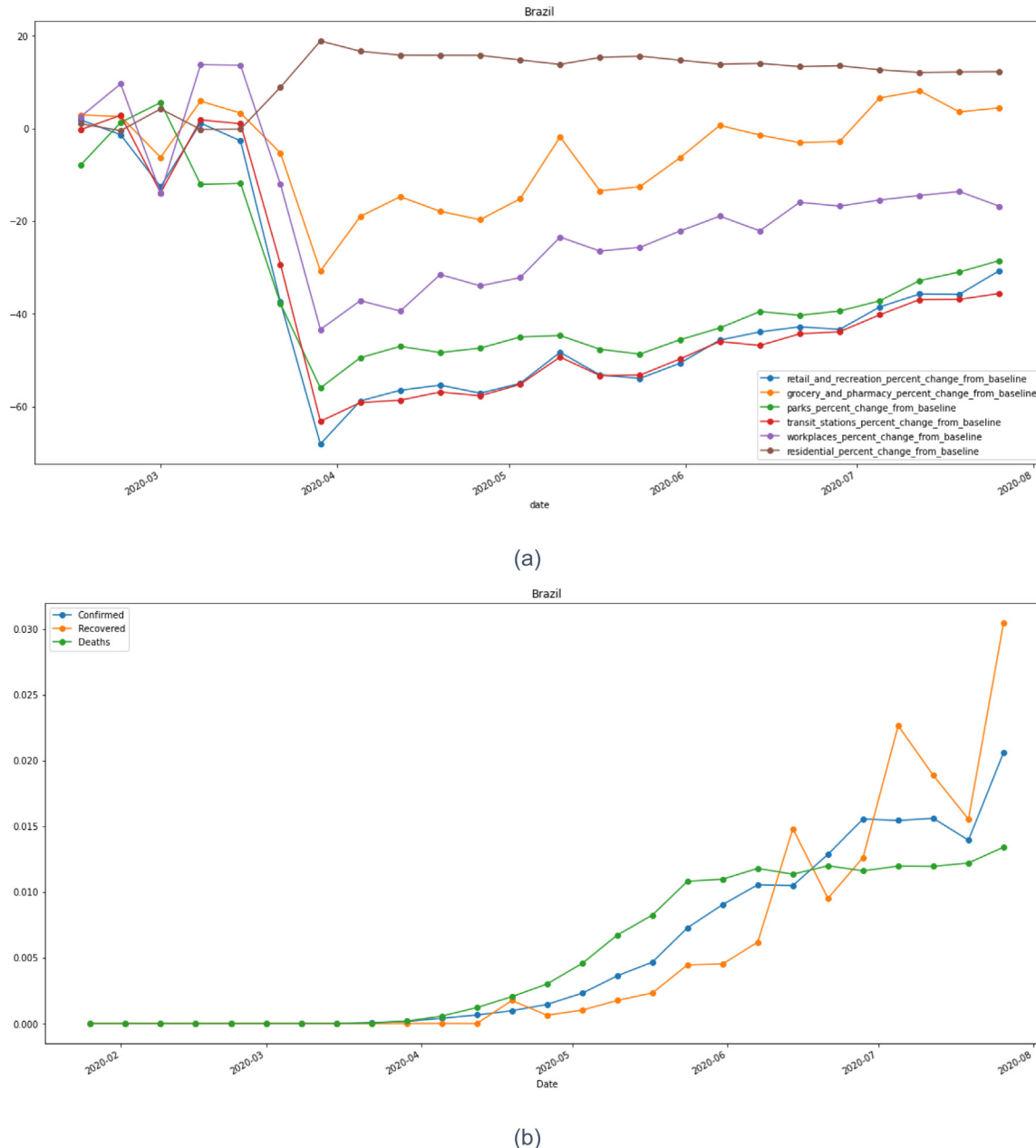


**Fig. 2.** (a) Human mobility dynamics in Brazil (b) Weekly mean confirmed cases in Brazil (c) Human mobility dynamics in Malaysia (d) Weekly mean confirmed cases in Malaysia (e) Human mobility dynamics in Indonesia (f) Weekly mean confirmed cases in Indonesia.

the Earth's surface integrated over the day and taking the UV radiation's attenuation due to clouds. The cloud data is compiled from the geostationary Meteosat Second Generation (MSG) observations. The UV dose is computed for three different action spectra, i.e., for three other health effects: erythema (sunburn) of the skin (UVDEF), vitamin-D production in the skin (UVDVF), and DNA-damage (UVDDF).

Government stringency is related to the measurement provided by the Oxford COVID-19 Government Reaction Tracker [24]. The Tracker includes 100 Oxford community individuals who have ceaselessly upgraded a database of 17 parameters of government response. These parameters look at control approaches such as school and working environment closings, open occasions, open transport, and stay-at-home policies. The Stringency Record could be a number from 0 to 100 that reflects these indicators. The higher score shows a better level of stringency. Stringency list gives a picture of the policies at which any nation

implemented its most grounded measures. Some countries have had their deaths continue to flatten only as they have hit their hardest stringency, such as Italy, Spain, or France. As China took harder than initial stringency, its death curve was flattened.

## 2.2. UV index dynamics as environmental factors

The UV index (UVIEF) is derived from the measured solar radiation in the UV spectra that arrives on the surface. It is calculated by considering the proportional contribution of UV-A and UV-B, two of the three-wavelength based types of UV radiation. UV-A is characterized as the UV radiation of which the wavelength ranges from 280–315 nm, while the wavelength of UV-B is between 315 nm and 400 nm. UV spectra are captured by the Global Atmosphere Watch (GAW) station. In this study, the daily mean UV index (0–17) and daily mean Ozone (Dobson Unit) are considered as parameters involved in the correlation

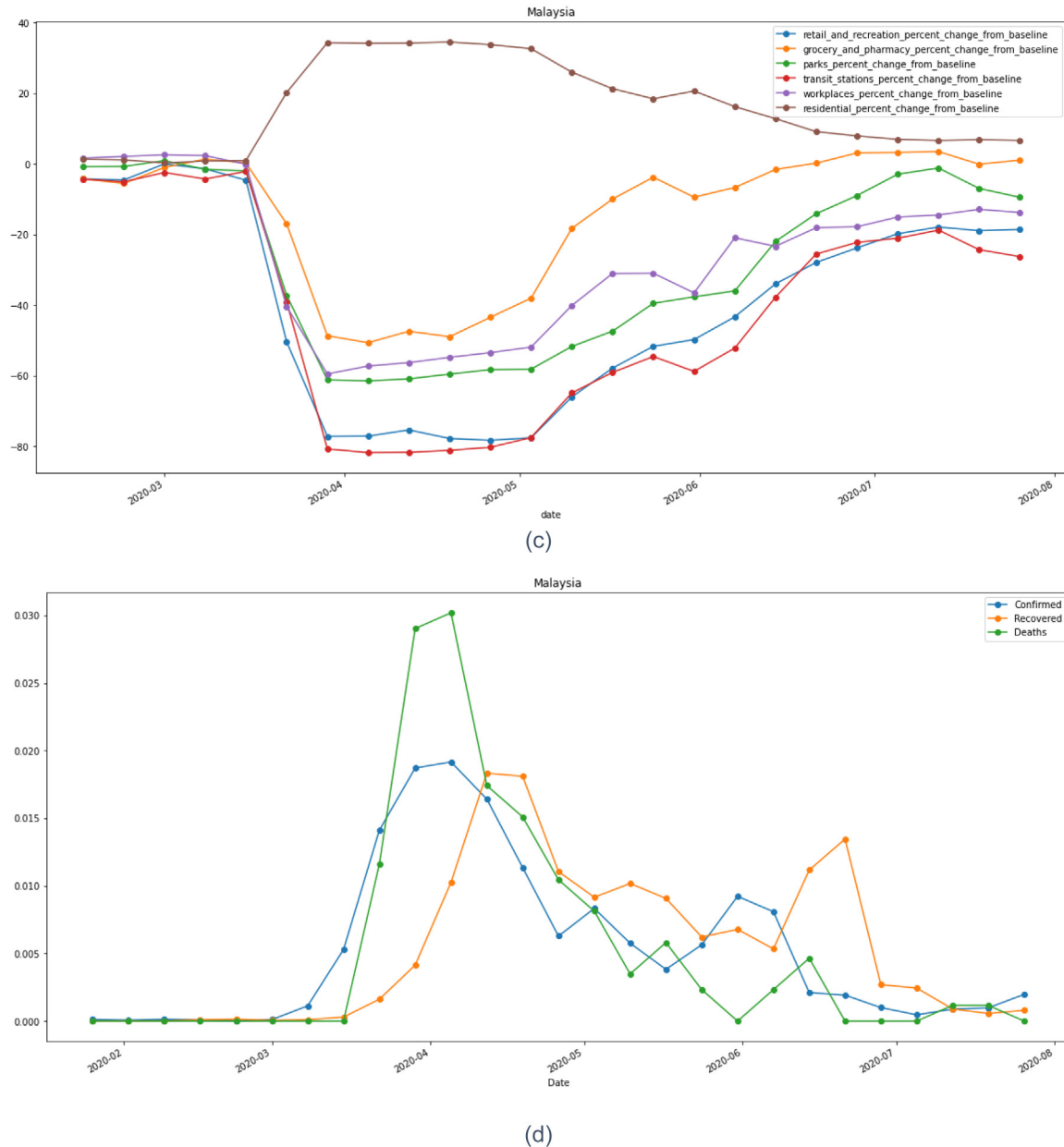


Fig. 2. (continued).

analysis. The depletion of the protective stratospheric ozone layer due to chlorofluorocarbons (CFCs) and halons has increased UV radiation. The UV index is measured under the assumption of a clear sky without any barriers such as clouds. The trade-offs between 3 geographical locations (northern subtropical, tropical, and southern subtropical areas) are investigated in terms of how UV index and COVID-19 are related over time. The selected GAWs are located in Argentina, Australia, Chile, and Brazil (Sao Paulo) for southern subtropical countries. For tropical countries, GAWs of India, Saudi Arabia, and Thailand are selected as representative countries. Finally, GAWs of Germany, Italy, Japan, Russia, Spain, and Taiwan are selected to represent northern subtropical countries. The duration UV index time series is from 2020/01/22 to 2020/07/20. The time-series data are then transformed into a weekly mean series to capture the bigger picture of dynamics.

Fig. 1a, 1b, and 1c show pandemic growth in tropical (green), northern subtropical (blue), and southern subtropical (red) countries for confirmed, recovered, and death cases, respectively. Note that the number of confirmed cases, recovered, and deaths are

normalized across all countries. Since the end of March, the blue countries grew over time and faster than the green and red countries. The green countries grew sharper and faster than red countries, even though there were cross points in the middle of growth. The overtaking points indicate a growth pace that is becoming slower than the other, and vice versa. This dynamical pace happened between two adjacent groups, either blue with green or green with red. Blue countries were starting to converge, and conversely, red countries were starting to emerge both at the beginning of May even though outlier countries exist. These phenomena possibly can be explained in Fig. 1d where daily mean UV index in red countries were monotonically decreasing as the winter comes and the opposite for blue countries. It can be suggested that there is an indication that COVID-19 is a seasonal pandemic depending on geographical locations.

During summer, UV can inactivate viruses that live in the air and on the surface of the objects especially at noon in tropical or subtropical countries. However, it may not be significant in closed spaces like workspace and areas with the intensive

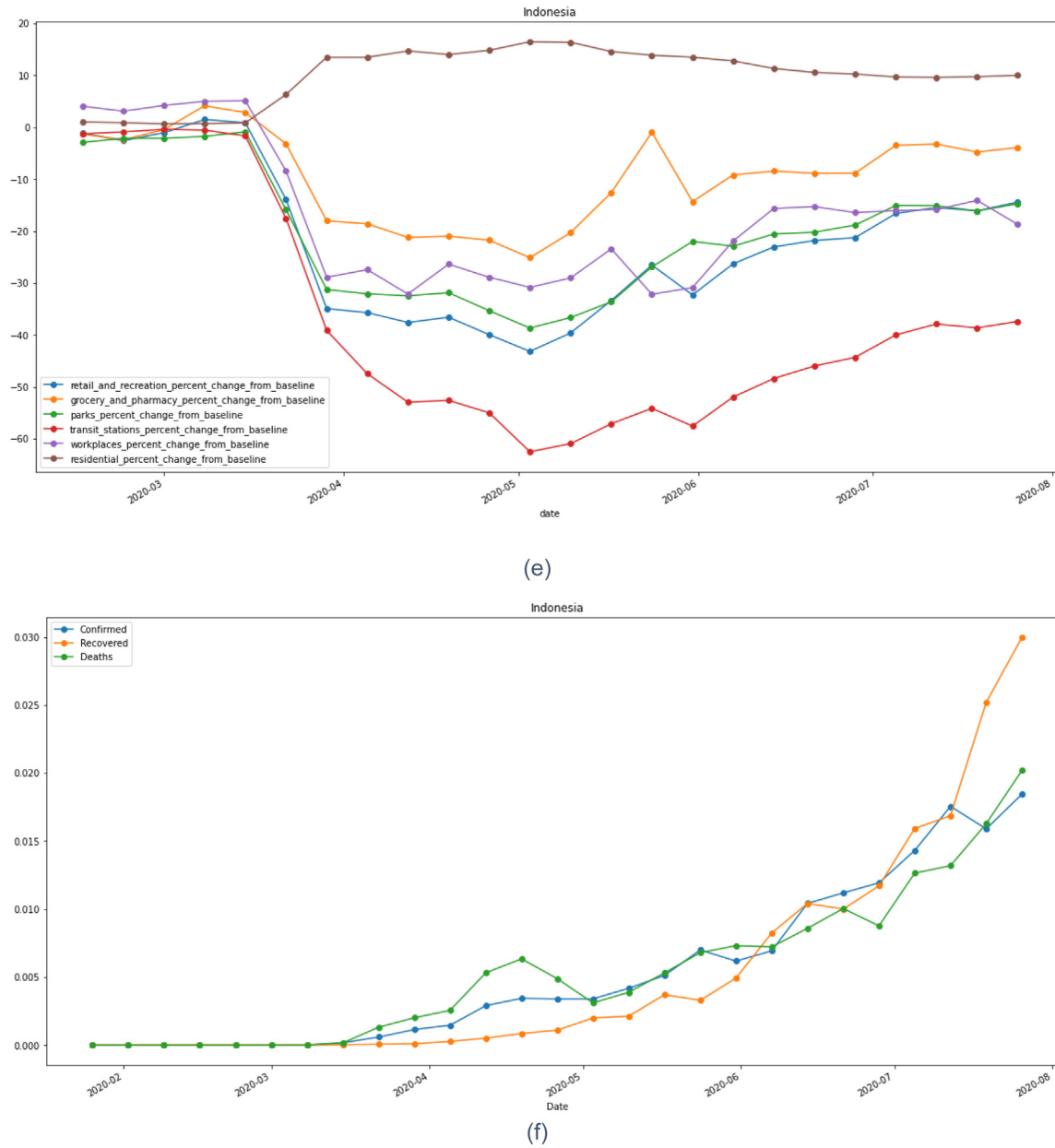


Fig. 2. (continued).

human-to-human transmission, especially in densely populated areas. Different COVID-19 pandemic growth patterns in northern subtropical, southern subtropical and tropical countries occur over time.

### 2.3. Human mobility dynamics as behavioral factors

Human mobility dynamics are movement trends over time by geography, across different categories of places such as retail and recreation, groceries and pharmacies, parks, transit stations, workplaces, and residential [25]. It sees how your community is moving around differently due to COVID-19. The key drivers to be used in human mobility analysis are community activities dynamics during a pandemic depending on geographical locations (focusing on tropical countries). After the first outbreak, human mobility has changed from before pandemic due to lockdown or outdoor activity restriction from the government. To see the effect of these restrictions, we investigate activities dynamics relative to COVID-19 growth. To realize this, Google Mobility

data [25] that provide six different activities are utilized. Those activities are grocery and pharmacy, workplaces, transit stations, retail and recreation, residential, and parks percent change from baseline. To see the effect of reducing activities intensity, we analyze the time-lagged correlation between activities dynamics and COVID-19 growth. It means that the impact of activities reductions on COVID-19 growth patterns after several days is temporally investigated. The countries to be investigated in this study are India, Brazil, Malaysia, Saudi Arabia, Indonesia, and Thailand (tropical countries).

**Fig. 2a** shows that human mobility in Brazil reached the lowest activities percent change to baseline in the middle of April 2020 and then gradually increased its percentage of change to baseline over time. The increasing phenomena reveal the new normal life has been adapted. **Fig. 2b** shows weekly mean confirmed cases in Brazil that grew since the middle of April 2020. Note that the number of confirmed cases here has been normalized across all countries considered in this dataset. **Fig. 2c** shows that Malaysia's human mobility reached the lowest activity of retail

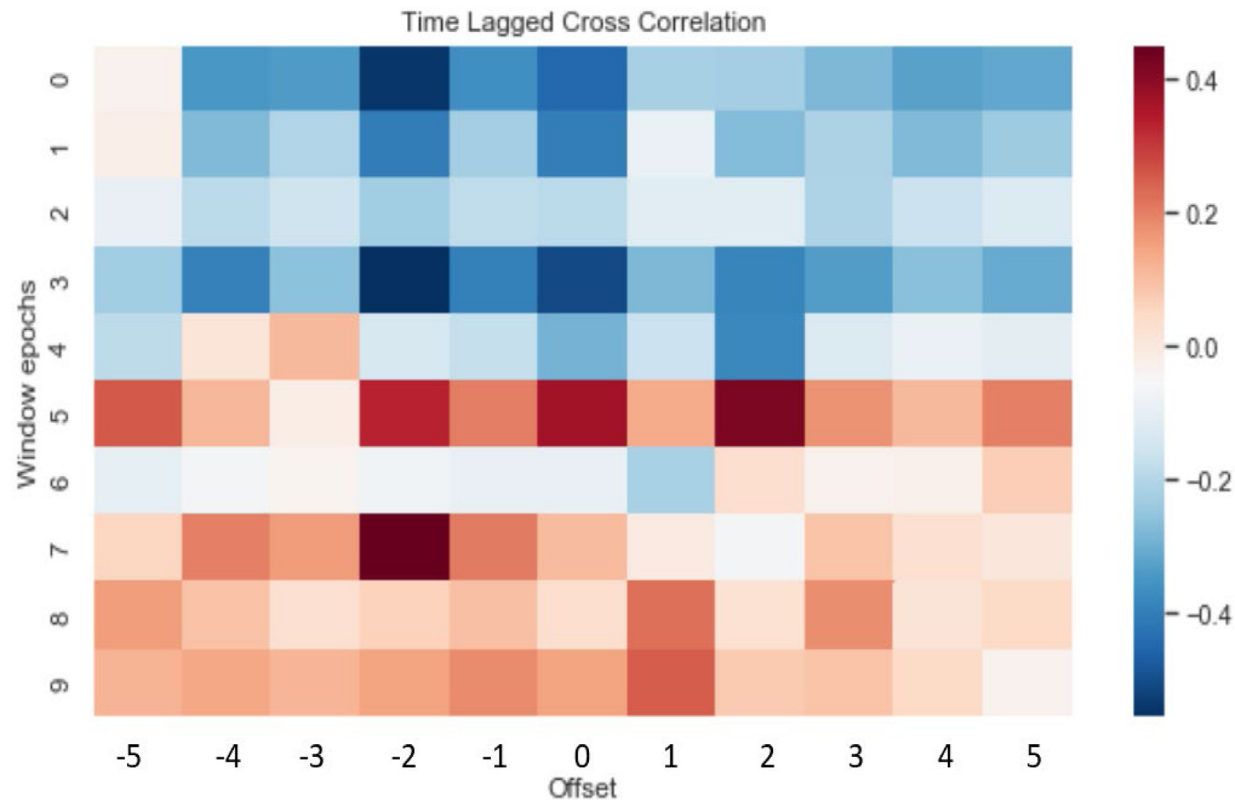


**Fig. 3.** Time lagged cross-correlation between weekly mean confirmed cases and human activities in Jakarta region.

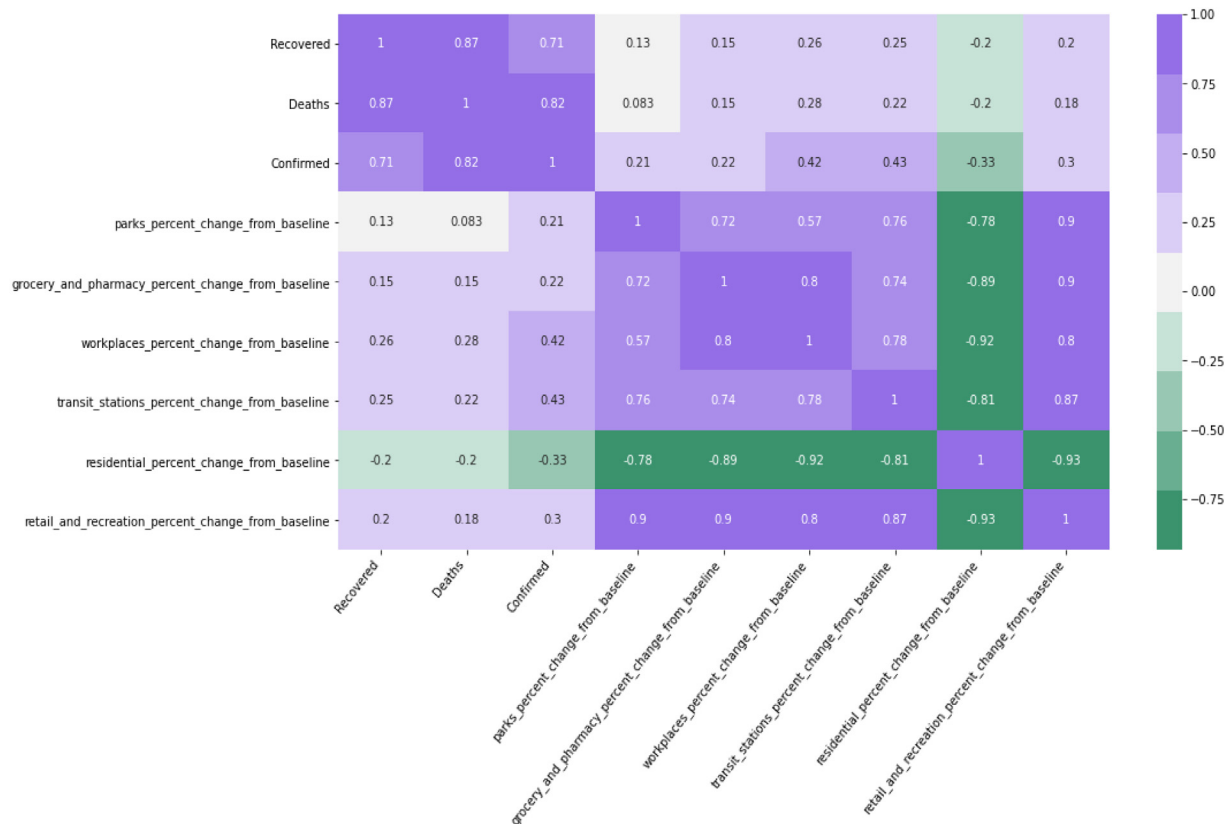


**Fig. 4.** Pearson correlation of weekly mean confirmed, recovered, death cases and weekly mean human activities of all countries with off set of -2.

**Table 1**

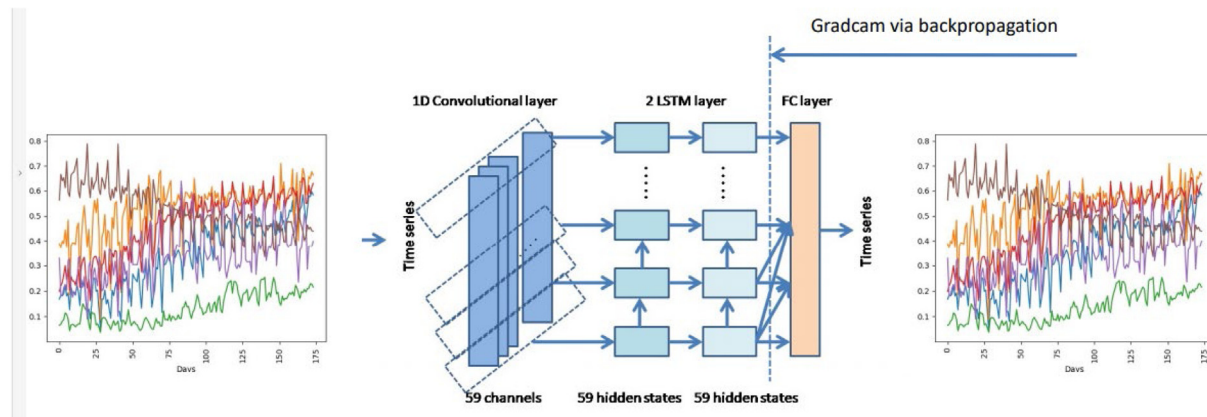
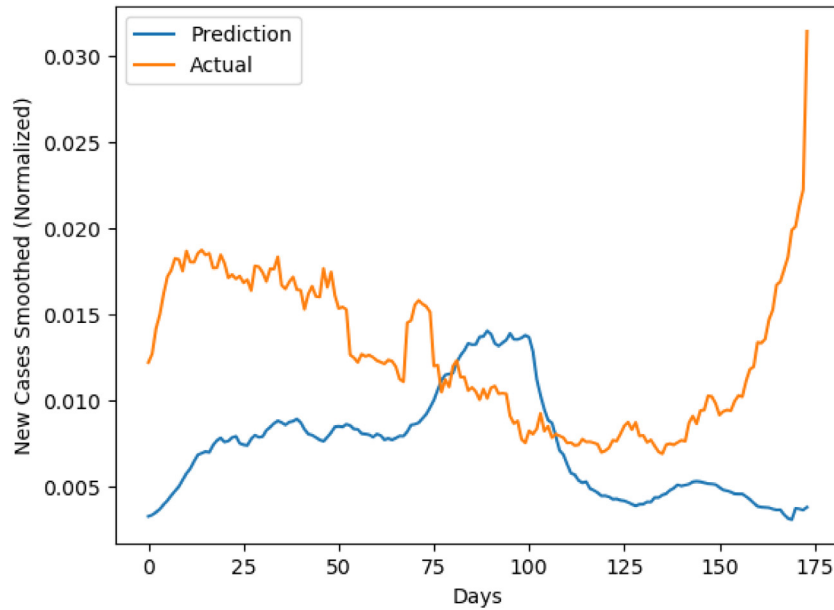
59 factors used in this research ranging from environmental, government, economical, to behavioral factors during 2020-03-22 to 2020-09-11.

| Number | Factor   | Category            | Value  |
|--------|--|---------------------|--|
| 1      | retail_and_recreation_percent_change_from_baseline | Behavioral/Mobility | Percentage   |
| 2      | grocery_and_pharmacy_percent_change_from_baseline  | Behavioral/Mobility | Percentage   |
| 3      | parks_percent_change_from_baseline                 | Behavioral/Mobility | Percentage   |
| 4      | transit_stations_percent_change_from_baseline      | Behavioral/Mobility | Percentage   |
| 5      | workplaces_percent_change_from_baseline            | Behavioral/Mobility | Percentage   |
| 6      | residential_percent_change_from_baseline           | Behavioral/Mobility | Percentage   |
| 7      | total_cases  | COVID-19            | Number of people   |
| 8      | new_cases  | COVID-19            | Number of people   |
| 9      | new_cases_smoothed                                 | COVID-19            | Number of people smoothed  |
| 10     | total_deaths                                       | COVID-19            | Number of people   |
| 11     | new_deaths   | COVID-19            | Number of people   |
| 12     | new_deaths_smoothed                                | COVID-19            | Number of people smoothed  |
| 13     | total_cases_per_million                            | COVID-19            | Number of people per million   |
| 14     | new_cases_per_million                              | COVID-19            | Number of people per million   |
| 15     | new_cases_smoothed_per_million                     | COVID-19            | Number of people smoothed per million                                      |
| 16     | total_deaths_per_million                           | COVID-19            | Number of people per million   |
| 17     | new_deaths_per_million                             | COVID-19            | Number of people per million   |
| 18     | new_deaths_smoothed_per_million                    | COVID-19            | Number of people per thousand per million                                  |
| 19     | new_tests  | COVID-19            | Number of people   |
| 20     | total_tests  | COVID-19            | Number of people   |
| 21     | total_tests_per_thousand                           | COVID-19            | Number of people per thousand  |
| 22     | new_tests_per_thousand                             | COVID-19            | Number of people per thousand  |
| 23     | new_tests_smoothed                                 | COVID-19            | Number of people smoothed  |
| 24     | new_tests_smoothed_per_thousand                    | COVID-19            | Number of people per thousand  |
| 25     | tests_per_case                                     | COVID-19            | Percentage   |
| 26     | positive_rate                                      | COVID-19            | Percentage   |
| 27     | tests_units  | COVID-19            | People tested or not   |
| 28     | stringency_index                                   | Government          | 0–100  |
| 29     | Population   | Demography          | Number of people within country  |
| 30     | population_density                                 | Demography          | Number of people within country per km <sup>2</sup>                        |
| 31     | median_age   | Demography          | Age  |
| 32     | aged_65_older                                      | Demography          | Percentage   |
| 33     | aged_70_older                                      | Demography          | Percentage   |
| 34     | gdp_per_capita                                     | Economic            | Gross domestic product per capita (Purchasing Power Parity)                |
| 35     | extreme_poverty                                    | Economic            | Percentage   |
| 36     | cardiovascular_death_rate                          | Health              | The annual number of deaths from cardiovascular diseases per 100000 people |
| 37     | diabetes_prevalence                                | Health              | Percentage   |
| 38     | female_smokers                                     | Health              | Percentage   |
| 39     | male_smokers                                       | Health              | Percentage   |
| 40     | handwashing_facilities                             | Health Facilities   | Number of hand washing facilities  |
| 41     | hospital_beds_per_thousand                         | Health Facilities   | Number of hospital beds per thousand                                       |
| 42     | life_expectancy                                    | Health              | Age  |
| 43     | human_development_index                            | Education           | 0–1  |
| 44     | UVIEF (cloud-free UV index)                        | Environmental       | 0–17   |
| 45     | UVIEFerr (cloud-free erythemal UV index smoothed)  | Environmental       | kJ/m <sup>2</sup>  |

(continued on next page)

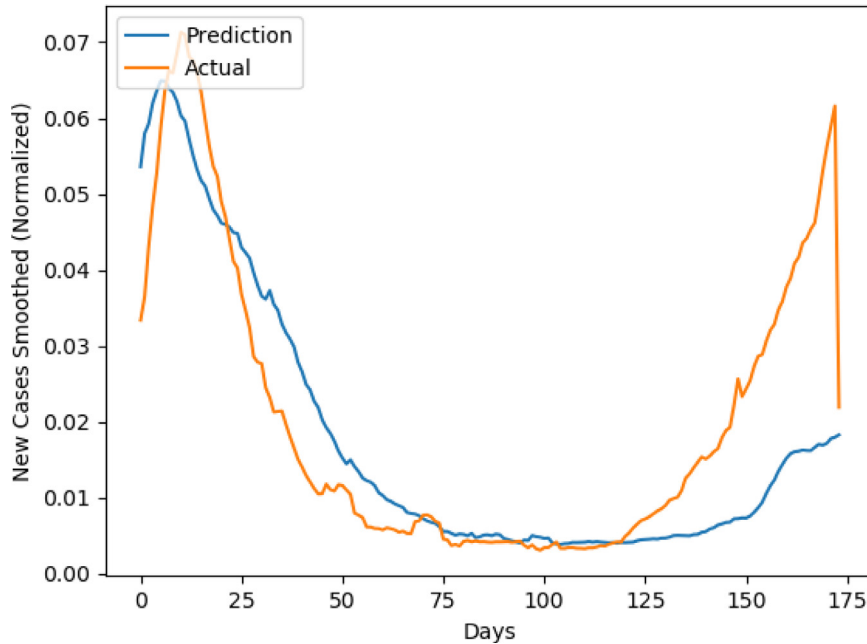
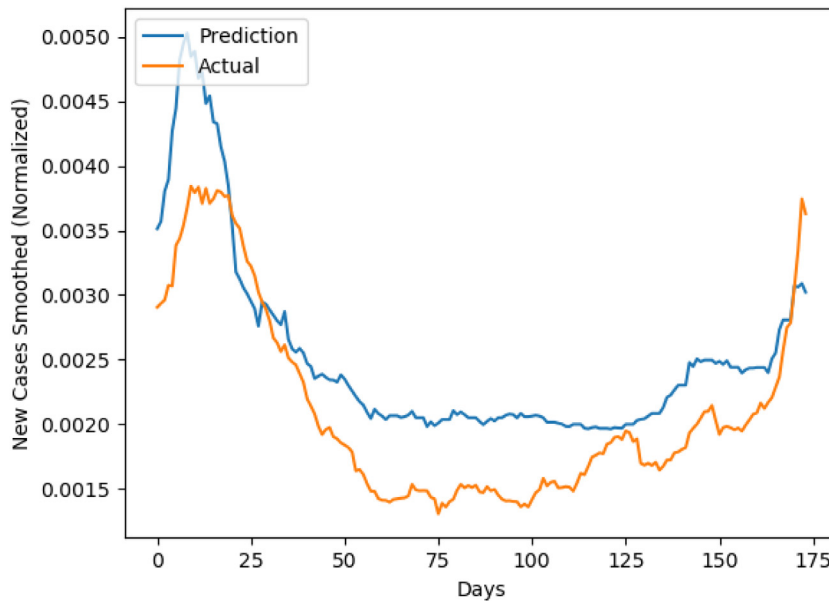
**Table 1** (continued).

| Number | Factor   | Category      | Value             |
|--------|--|---------------|-------------------|
| 46     | UVDEF (cloud-free erythemal UV dose)                 | Environmental | kJ/m <sup>2</sup> |
| 47     | UVDEFerr (cloud-free erythemal UV dose smoothed)     | Environmental | kJ/m <sup>2</sup> |
| 48     | UVDEC (cloud-modified erythemal UV dose)             | Environmental | kJ/m <sup>2</sup> |
| 49     | UVDECerr (cloud-modified Vitamin-D UV dose smoothed) | Environmental | kJ/m <sup>2</sup> |
| 50     | UVDVF (cloud-free vitamin-D UV dose)                 | Environmental | kJ/m <sup>2</sup> |
| 51     | UVDVFerr (cloud-free vitamin-D UV dose smoothed)     | Environmental | kJ/m <sup>2</sup> |
| 52     | UVDVC (cloud-modified vitamin-D UV dose)             | Environmental | kJ/m <sup>2</sup> |
| 53     | UVDVCerr (cloud-modified vitamin-D UV dose smoothed) | Environmental | kJ/m <sup>2</sup> |
| 54     | UVDDF (cloud-free dna-damage)                        | Environmental | kJ/m <sup>2</sup> |
| 55     | UVDDFerr (cloud-free dna-damage smoothed)            | Environmental | kJ/m <sup>2</sup> |
| 56     | UVDDC (cloud-modified dna-damage)                    | Environmental | kJ/m <sup>2</sup> |
| 57     | UVDDCerr (cloud-modified dna-damage smoothed)        | Environmental | kJ/m <sup>2</sup> |
| 58     | CMF (average cloud modification factor)              | Environmental | –                 |
| 59     | Ozone (local solar noon ozone column)                | Environmental | DU (Dobson Unit)  |

**Fig. 5.** Convolution-LSTM architecture and its visual attribution via Gradcam.**Fig. 6.** Actual and reconstruction of Indonesia.

and recreation percent change to baseline in the middle of May 2020 and then gradually increased its percentage of change to baseline. The duration of low activities was around a month, starting from the middle of April to May 2020. After May, the

increasing activities were recorded, revealing new normal life has been adapted. Fig. 2d shows weekly mean confirmed cases in Malaysia grew starting from the middle of March 2020. However, starting from May 2020, the weekly mean confirmed cases were

**Fig. 7.** Actual and reconstruction of Norway.**Fig. 8.** Actual and reconstruction of Italy.

decreasing. Note that the number of confirmed cases here has also been normalized across all countries considered in this dataset. Fig. 2e shows that Indonesia's human mobility reached the lowest activities percent change to baseline in the middle of May 2020 and then gradually increased its percentage of change to baseline. The increasing phenomena show that the new normal life has been adapted. Fig. 2f shows weekly mean confirmed cases in Indonesia that grew exponentially since the end of March 2020 as the number of tests increased. Note that the number of confirmed cases here also has been normalized across all countries considered in this dataset.

To answer the question of whether there is any correlation between the decreasing activities before new normal and weekly mean confirmed cases after the new normal, time-lagged cross correlation was carried out.

#### 2.4. Statistical analysis

The investigation of cross-correlation in Jakarta region in Fig. 3 showed a strong positive correlation when weekly mean confirmed cases time series are correlated with weekly mean human activities with an off set of  $-2$ . The weekly mean confirmed cases strongly relate to weekly mean human activities after around two weeks.

Based on the investigation in Fig. 4, we conducted a correlation test of all countries between weekly mean confirmed, recovered, and death cases with weekly mean human activities with an offset of  $-2$  (2 weeks before). It can be concluded that weekly mean confirmed cases are positively correlated to weekly mean workplaces and transit stations percent change from baseline by 0.42 and 0.43 with correlation  $p$ -value of 0.003 and 0.002, respectively. Weekly mean confirmed cases are negatively correlated to

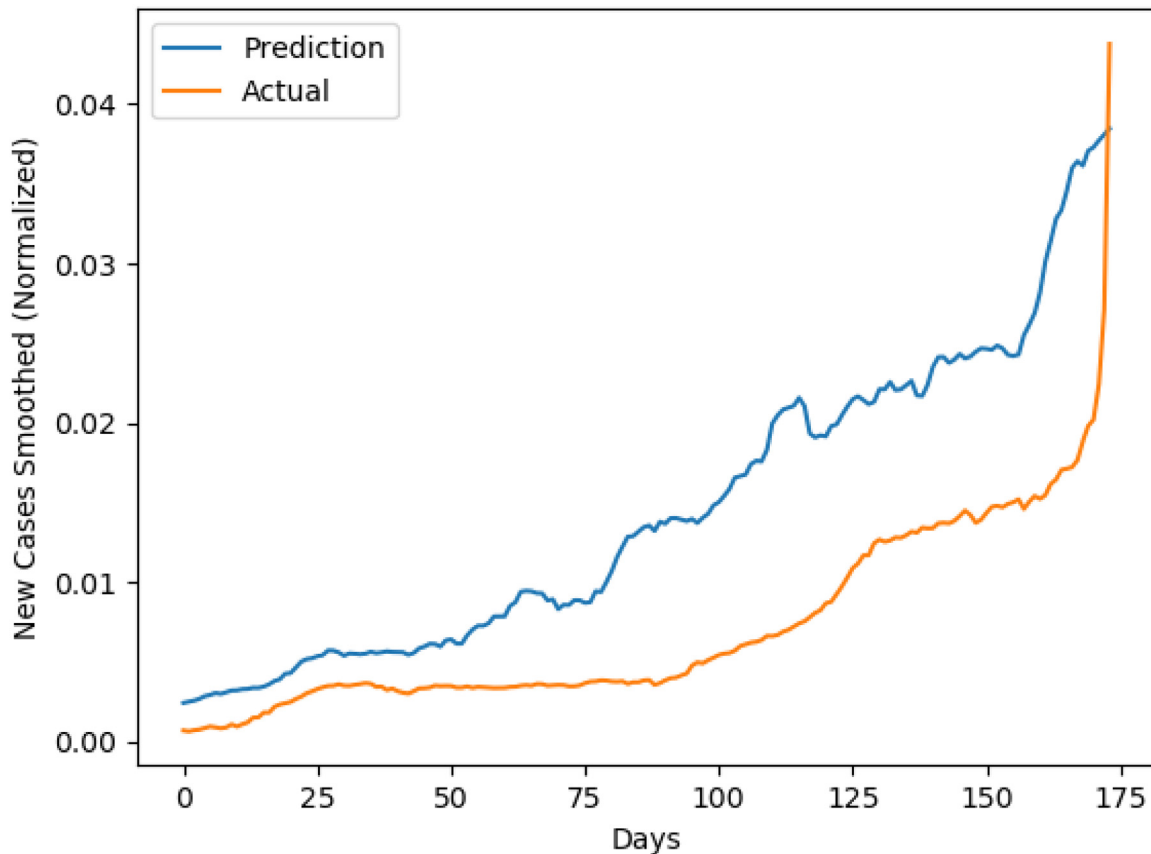


Fig. 9. Actual and reconstruction of Sweden.

weekly mean residential percent change from baseline by  $-0.33$  with a correlation  $p$ -value of  $0.03$ . It means that weekly mean confirmed cases correlate to weekly mean workplaces, transit stations, and weekly mean residential percent change from baseline with statistically significant ( $p < 0.05$ ).

#### 2.5. Multivariate time series analysis via explainable deep neural network

In this research, multivariate time series data set of 59 factors from 55 countries is employed. It consists of six behavioral, 21 COVID-19, one government, two geographical, three morphological, two economics, five health related factors, two health facilities, one education, and 16 environmental categories. Each factor is captured daily, except environmental factors (UVs) are represented by daily mean observations. A variant of DNNs called Long Short Term Memory (LSTM) [26] is trained to predict the outcome series of daily 59 factors over 174 days (2020-03-22 to 2020-09-11). All features in the X dataset are normalized feature-wise into following equation (Eq. (1)):

$$\hat{X} = \frac{X - X_{min}}{X_{max} - X_{min}} \quad (1)$$

To achieve explainable prediction of Spatio-temporal data, we develop a Convolution-LSTM model that consists of 1D convolution layer and 2 LSTM layers with 59 hidden states followed by a fully connected layer (FC) with Sigmoid activation (Fig. 4). The whole of LSTM units contains the input gate, the forget gate, and the output gate to capture spatio-temporal correlation and dynamics of multivariate time-series data. The forward propagation flows from input layer, hidden layers, and output layer followed by Sigmoid activation.

**Table 2**  
Parameters of proposed Conv-LSTM.

| Layer               | Value   |
|---------------------|---|
| Input layer         | (length, features)=(174,59)                     |
| Convolution layer   | 59 filters, size= $1 \times 7$ kernel, stride=3 |
| LSTM layer 1        | (input, hidden unit)=(59,59)                    |
| LSTM layer 2        | (input, hidden unit)=(59,59)                    |
| FC layer            | (input,output)=(59 $\times$ 56,174 $\times$ 59) |
| Activation function | Sigmoid   |
| Output layer        | (length, features)=(174,59)                     |

As shown in Table 2, our proposed Conv-LSTM consists of the input layer with temporal length of 174 with 59 features, a convolution layer of 59 channel with filter size of  $1 \times 7$  each, 2 LSTM layers each of which has an input channel of 59 and an output channel of 59. Finally, FC layer with an input size of  $59 \times 56$  and an output size of  $174 \times 59$  followed by the Sigmoid activation function is utilized. With an output layer size of 174 in temporal length and 59 in number of features, this architecture is purposely used for the explanation of long-range multivariate time series. Based on the architecture, our proposed model is different from the usual Conv-LSTM [27] which is purposely designed for training a sequence of stacked images. Moreover, from the perspective of output size, our Conv-LSTM aims to predict a long-range time series to obtain an explanation of multivariate temporal prediction rather than only a single value prediction [28,29].

After the learning phase, gradient-based optimization via back-propagation is utilized from which attribution maps (saliency maps) are generated. The visual attribution extracts attention to features that relevant to final spatio-temporal time-series predictions (Fig. 5). Specifically, the method called GradCAM [30]

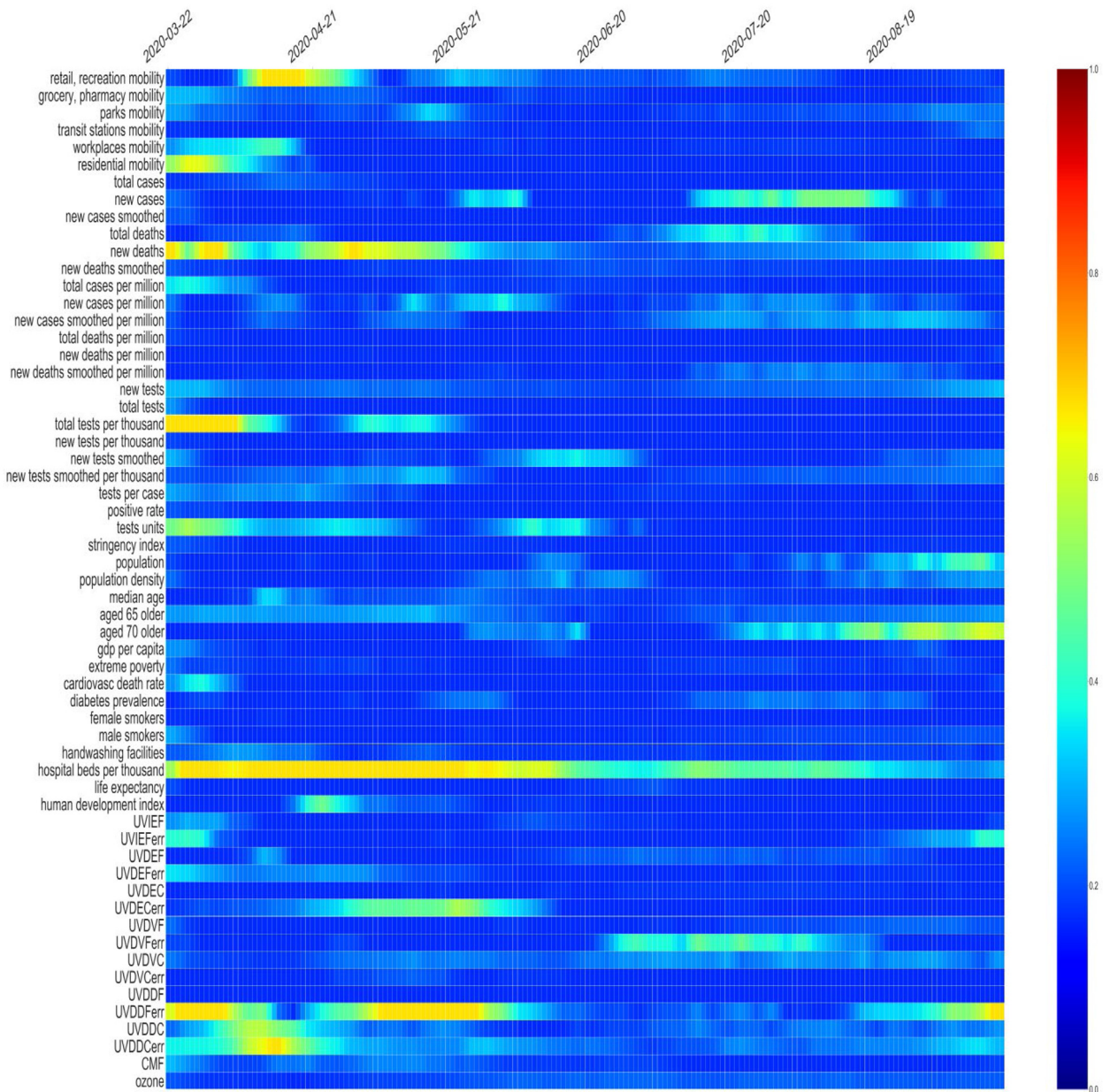


**Fig. 10.** Time and feature attention corresponding to a prediction for new daily COVID-19 cases in Italy.

is used to create its attribution maps. Grad-Cam is applied to the last hidden layer where its output activation is weighted with important weight associated with time-series predictions followed by Rectified Linear Unit (ReLU) activation.

The formulation of Gradcam for LSTM hidden layer is given in Eq. (2) as follows:

$$\text{Att} = \text{ReLU} \left( \frac{\partial \hat{p}_{\text{new\_cases\_smoothed}}}{\partial \text{sigmoid}(\text{out}_{\text{LSTM\_2}})} \frac{\partial \text{sigmoid}(\text{out}_{\text{LSTM\_2}})}{\partial \text{out}_{\text{LSTM\_2}}} \text{out}_{\text{LSTM\_2}} \right) \quad (2)$$

Where  $\text{Att}$ ,  $\hat{p}_{\text{new\_cases\_smoothed}}$  and  $\text{out}_{\text{LSTM\_2}}$  are visual attribution, reconstruction output containing 59 factors, reconstruction output containing only new cases smoothed, and output of hidden layer of the second layer of LSTM (features), respectively. The gradients are obtained through partial derivatives and chain rule. The final visual attribution is transformed into clean visualization using ReLU activation by eliminating negative values.

### 3. Experimental setup

This multidimensional study uses 3 data sets of COVID-19 growth and its attribution, UVs, and people mobility data. The time-series data was taken from 2020-03-22 until 2020-09-11. The selected countries are located in tropical, northern subtropical, and southern subtropical regions. Data sets of worlds confirmed COVID-19, UV index, pollution, and people mobility time series were taken from Ourworldindata [31], Tropospheric Emission Monitoring Internet Service (TEMIS) [32], and Google Mobility [25], respectively. Specific data, like UV index and pollution in Jakarta, Indonesia, were taken from Indonesia Meteorology, Climatology, and Geophysical Agency (BMKG). Confirmed, recovered, and death cases of COVID-19 data in Jakarta have been obtained from the Indonesia Ministry of Health.

The aforementioned data set references can be accessed to investigate the detailed definition of each factor. There are 55 countries at various scales of geographical area and population

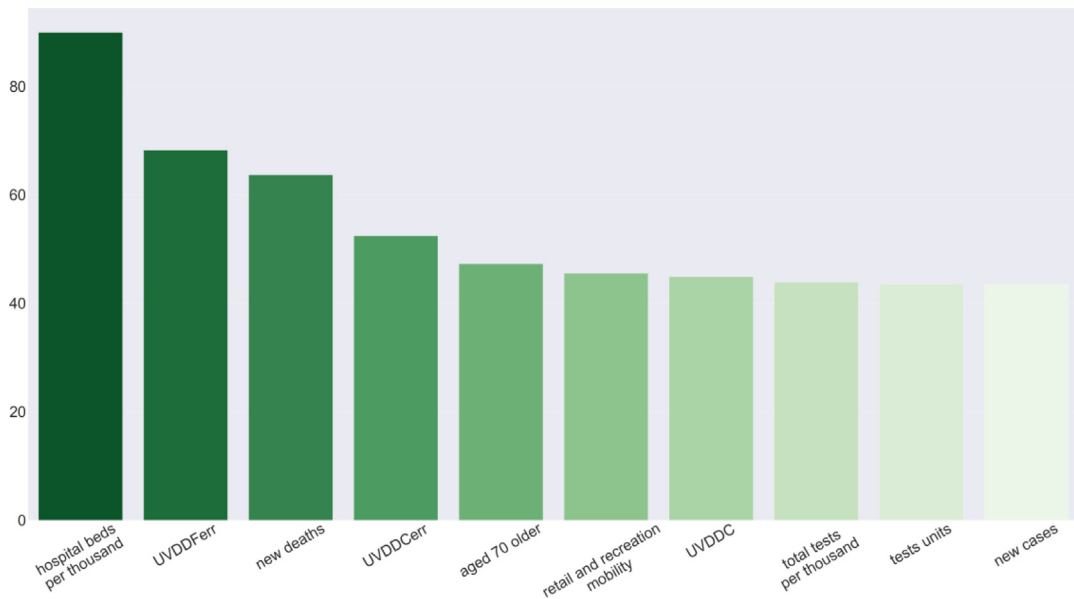


Fig. 11. Temporal aggregation of attribution in Italy (x-axis is variables and y-axis is aggregation score).

**Table 3**  
Contribution of features to Conv-LSTM prediction in RMSE.

|  | Italy         | Sweden       | Indonesia    | Norway       |
|--|---------------|--------------|--------------|--------------|
| Without environmental features         | 0.001         | <b>0.007</b> | 0.017        | 0.026        |
| Without mobility (behavioral) features | 0.002         | 0.009        | <b>0.007</b> | 0.028        |
| All features                           | <b>0.0005</b> | 0.009        | 0.008        | <b>0.012</b> |

trained on DNNs to reveal its explanations. Note that all factors are normalized into the 0–1 range before feeding into DNNs.

We divide the dataset into training and validation, which are 55 and 4 countries, respectively. The total time-series length for all features is 174 days, 2020-03-22 to 2020-09-11. We use three architectures, which are a layer of 1D CNN, a layer of LSTM, and proposed Convolution-LSTM (Conv-LSTM), which are validated to test the data set using Root Mean Squared Error (RMSE). The number of epoch is set to 3000. We use Adam optimizer to update weights for each iteration with a learning rate of 0.001. The best architecture based on best validation score is selected as a visual explanation model.

#### 4. Results

Table 3 shows when tested without environmental features which consist of 'UVIEF', 'UVIEFerr', 'UVDEF', 'UVDEFerr', 'UVDEC', 'UVDECerr', 'UVDVF', 'UVDVFerr', 'UVDVC', 'UVDVCerr', 'UVDDF', 'UVDDFerr', 'UVDDC', 'UVDDCerr', and 'CMF', Italy and Norway got 0.001 and 0.002, respectively. All Features of Italy and Norway produce better prediction in terms of RMSE with 0.0005 and 0.12, respectively compared to without environmental features. When compared to without mobility features which consist of 'retail and recreation percent change from baseline', 'grocery and pharmacy percent change from baseline', 'parks percent change from baseline', 'transit stations percent change from baseline', and 'workplaces percent change from baseline', complete features obtain better RMSE. It reveals that mobility features are important for prediction especially in Norway and Italy. In Indonesia, without mobility features got better RMSE compared to without

**Table 4**  
Prediction accuracy (RMSE) of new cases of COVID-19 in Italy, Sweden, Indonesia, and Norway.

|                | Italy         | Sweden       | Indonesia    | Norway       |
|----------------|---------------|--------------|--------------|--------------|
| 1D CNN 1 layer | 0.052         | 0.134        | 0.085        | 0.069        |
| LSTM 1 layer   | 0.001         | 0.013        | 0.013        | 0.014        |
| Conv-LSTM      | <b>0.0005</b> | <b>0.009</b> | <b>0.008</b> | <b>0.012</b> |

environmental and complete features. However, when environmental features are not included, the prediction of new cases in Indonesia is even worse at 0.017 revealing environmental factors are more important in Indonesia. This condition is reversed in Sweden where mobility factors are more important for the dynamics of COVID-19 new cases prediction.

Table 4 shows the (Root Mean Squared Error) RMSE to validate model architectures to predict the time-series outcome of Italy, Sweden, Indonesia, and Norway. The low RMSE indicates that the prediction accuracy of validation is high and impacts reliable feature attribution. After predictions, spatio-temporal feature attention inside the Convolution-LSTM network can be visualized. High attention is represented by red color and gradually becomes blue as the attention value is decreased. The range of feature attention degrees is in the range of 0 to 1.

Fig. 6 shows the reconstruction and actual of new cases smoothed in Indonesia. Even though the reconstruction result hardly matches the pattern of the actual one, the RMSE is 0.008, which is the lowest compared to other models (Table 2). Improper reconstruction is due to presumably Indonesia is a large country with heterogeneous character and behavior. Compared to Sweden, Norway, or Italy, Indonesia is greater in terms of population, and geographic area, leading to the need for more detailed and complete data in terms of region and period. Another suggestion is by adding more countries to be fed into the model; thus model can generalize well and reduce overfitting. For future works, data to be analyzed should be more detailed in terms of the region and the time-series sample period.

Figs. 7, 8, and 9 show actual and reconstruction of new cases smoothed in Norway, Italy, and Sweden, respectively. They have a similar time-series pattern between actual and reconstruction and thus have a better outcome than Indonesia. Coincidentally, they are located in a similar geographical location of the northern subtropical area, which differs from Indonesia. It can be concluded

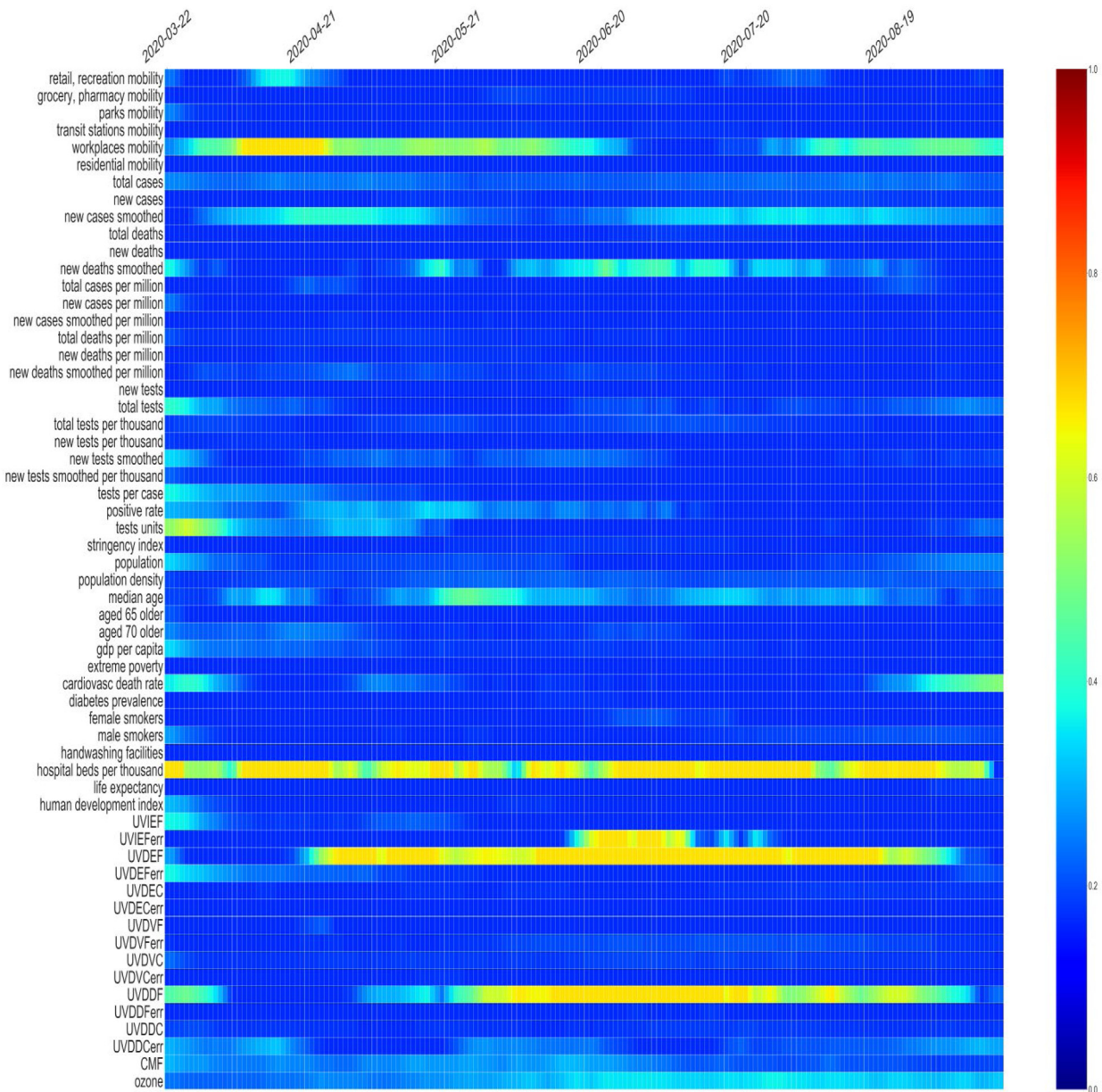


**Fig. 12.** Time and feature attention corresponding to a prediction for new daily COVID-19 cases in Sweden.

that more samples are necessary to generalize countries that have a similar pattern to Indonesia's COVID-19 case.

Fig. 10 shows the example of the visual attribution of Conv-LSTM prediction on a series of daily new COVID-19 cases in Italy. When the visual explanation is investigated, network put high attention on the residential, retail and recreation percent change from baseline at the beginning of time. It regards changing activity on those area contributes to the COVID-19 daily new cases pattern over the time in Italy. Total test per thousand, number of test units, and environmental factors of UVDDC and UVDDCerr at the beginning of time also influence the new cases over time. The number of aged 70 people at the end of the time contributes to the pattern of new cases growth over time. The number of hospital beds per thousand is linked over time by a network which suggests an important factor to be considered. Factors that have been put high attention at the beginning and the end of the time are the number of new deaths over time and environmental factor of UVDDFerr. Over time new cases smoothed follows environmental factor of UVDDFerr pattern which decreases at

the beginning of time and then increases again at the end of time. It indicates the influence of UV in affecting the graph of COVID-19 cases, especially in open spaces (the parks percent change from baseline influences new cases at the small amount at the beginning and the end of time) as the dynamics of UV in northern subtropical countries. In terms of the joint contribution of features, the network shows more attention to period between 2020-02-21 and 2020-04-21, which seems to correspond to residential mobility, daily new deaths, number of total tests per thousand, number of tests units, number of hospital beds per thousand, and UVDDFerr. Furthermore, the network also shows joint attention to between 2020-04-21 and 2020-05-21, which seems to correspond to retail and recreation mobility, daily new deaths, number of hospital beds per thousand, UVDECerr, and UVDDFerr.

Fig. 11 shows the rank of contribution band of variables when temporal information is aggregated in case of Italy. It shows that number of hospital bed has highest band revealing that it is dominant feature for daily new cases prediction in Italy.

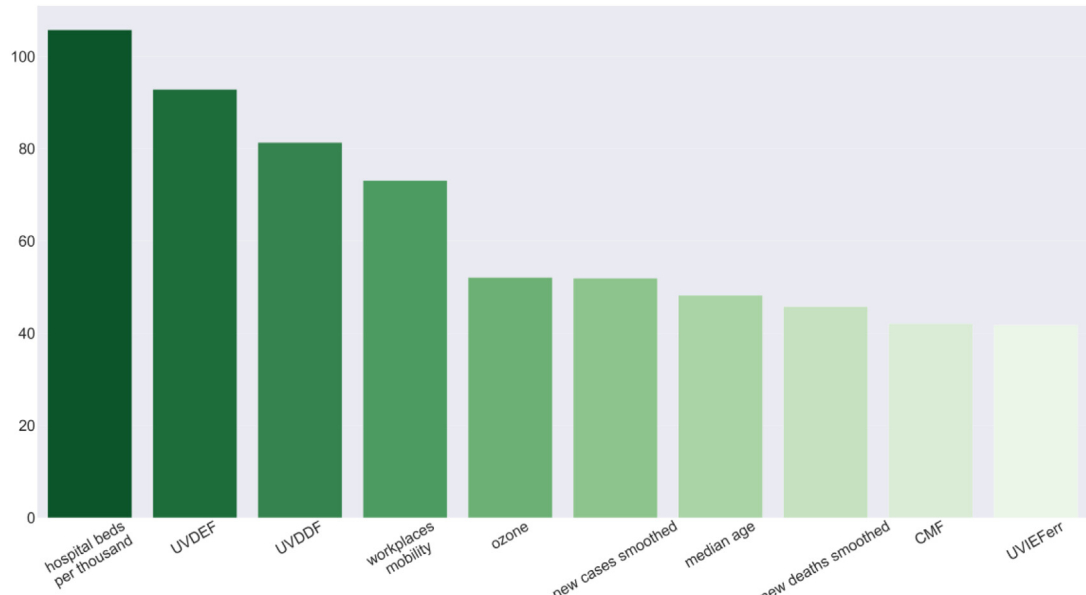


**Fig. 13.** Temporal aggregation of attribution in Sweden (x-axis is variables and y-axis is aggregation score).

The network also considers UVDDFerr, new deaths, UVDDCerr, aged 70 older, retail and recreation mobility, UVDDC, number of tests units, and number of new cases as contributing factors to time-series pattern of daily new cases. In terms of category, we figure out that the network's attention for Italy is spreading across health facility, environmental, demographic, mobility, and COVID-19 features.

Fig. 12 shows the visual attribution map of Conv-LSTM prediction on a series of daily new COVID-19 cases in Sweden. The Conv-LSTM network put attention into workplaces percent change from baseline almost the entire of the time while insufficient attention on other places. The number of test units influences new cases initially while median age people contribute in the middle of time. Cardiovascular death rate also is attributed by the network at the beginning and the end of the time. Same as Italy, the number of hospital beds per thousand gives significant contribution at the entire time. Environmental factors of UVIEFerr, UVDEF, and UVDDF affects new cases smoothed time series pattern in the middle of the time.

Temporally, attention to behavioral factors only highlights workplaces change to baseline over time. It regards open space as a park contributes to the COVID-19 daily new cases. UV index and dose increase over time in the northern subtropical countries toward summer. Correspondingly, the visual attribution also shows the degree of attention on environmental factors. It indicates the influence of UV on daily new COVID-19 cases, especially in open spaces like parks. The contribution of aged people is not as intense as Italy and Norway revealing Sweden's success in separating aged people and younger ones. In regards the joint contribution of features, the network highlights to period between 2020-05-21 and 2020-06-19 as joint attention, which seems to correspond to workplaces mobility, number of hospital beds per thousand, UVDEF, and UVDDF.

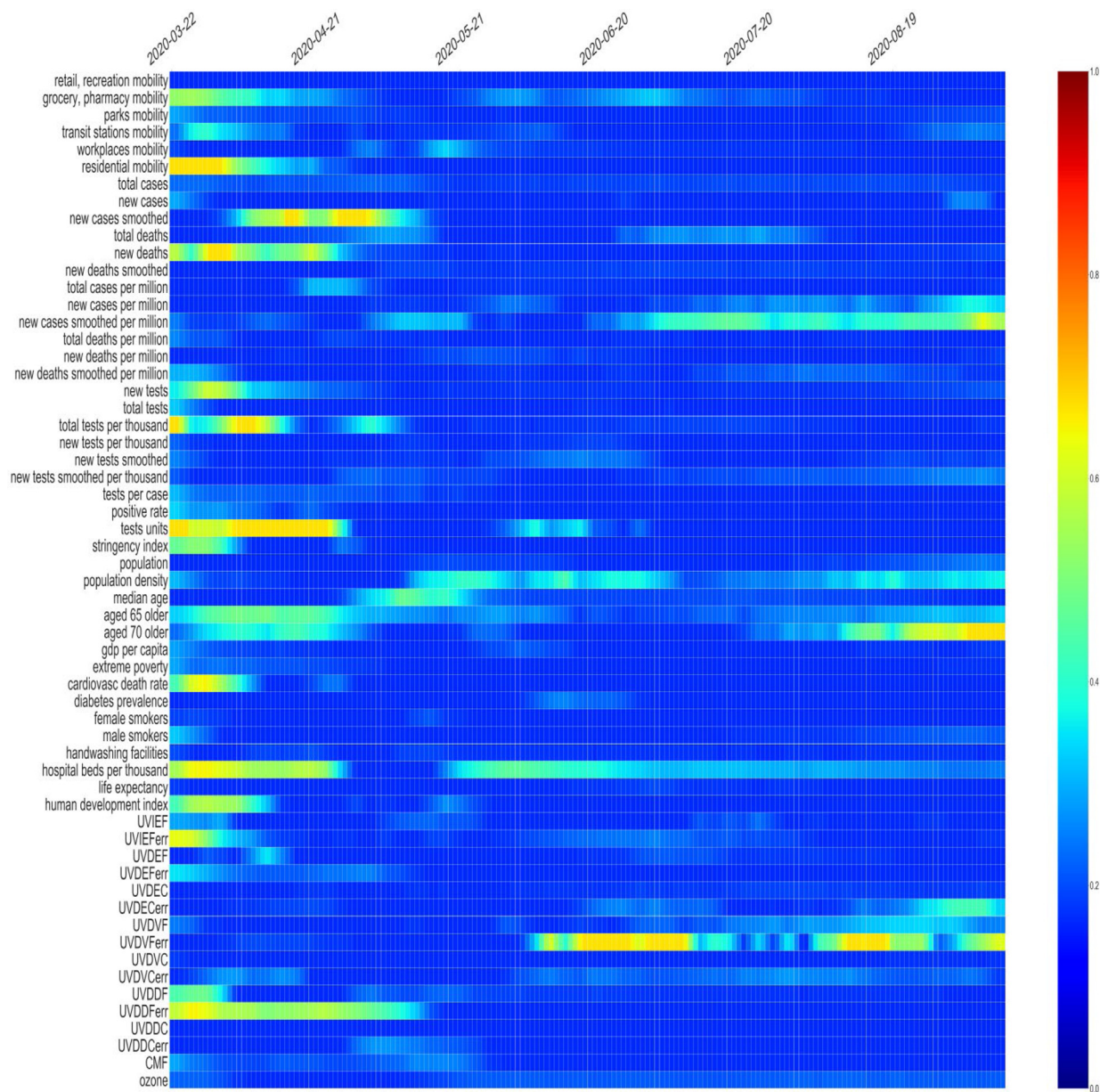
Fig. 13 shows the rank of contribution band of variables when temporal information is aggregated in case of Sweden. It shows that number of hospital bed has highest band revealing that it is dominant feature for daily new cases prediction in Sweden which is same as in Italy. The network also considers UVDEF, UVDDF, workplaces mobility, ozone, new cases smoothed, the number of median age, daily new death smoothed, CMF, and UVIEF as contributing factors to time-series pattern of daily new cases in

Sweden. We figure out that in category, the network's attention for Sweden is spreading across health facility, behavioral, environmental, demographic, and COVID-19 features.

Fig. 14 shows the example of the visual attribution map of Conv-LSTM prediction on series of daily new COVID-19 cases in Norway. Conv-LSTM network put attention into residential, grocery, and pharmacy percent change from baseline while insufficient attention on transit station percent change from baseline. It regards closed space contributes to the COVID-19 daily new cases. In Norway, the difference between Norway and Sweden is that closed space activities like in workplaces are not given as much attention as Sweden of contribution to daily new COVID-19 cases. It can be understood since the Sweden government's treatment of society is not as strict as Norway [33]. Visual attribution map also shows that government stringency is one of the critical factors contributing to daily new COVID-19 cases. Consequently, as shown in Figs. 7 and 9, Norway and Sweden have different new cases smoothed pattern over time where the former decreased and then increased while the latter is monotonically increasing. Besides, the number of test units, total tests per thousand, and the number of new tests initially affect the pattern of new cases smoothed over time.

The morphological demography factor of the number of aged 70 people at the end of time contributes to new cases smoothed. Human index and health factors of cardiovascular rate and number of hospital's bed are also factors that cannot be underestimated. Environmental factors like UVIEFerr, UVDVFerr, and UVDDFerr contribute to the new cases smoothed in Norway.

In Norway, the network shows more attention to period between 2020-02-21 and 2020-04-21 as the joint contribution of dominant features, which seems to correspond to grocery and pharmacy mobility, residential mobility, daily new deaths, number of total tests per thousand, number of tests units, stringency index, cardiovascular death rate, number of hospital beds per thousand, human development index, UVIEFerr, and UVDDFerr. It is interesting that different from the attribution map of Sweden which does not highlight stringency index, attribution map of Norway put attention to stringency index. Correspondingly, the government of Norway is stricter than Sweden in restricting community activities [33]. Furthermore, the network also shows joint attention to period after 2020-08-19, which seems to correspond to new cases smoothed per million, aged 70 older, and UVDVFerr.



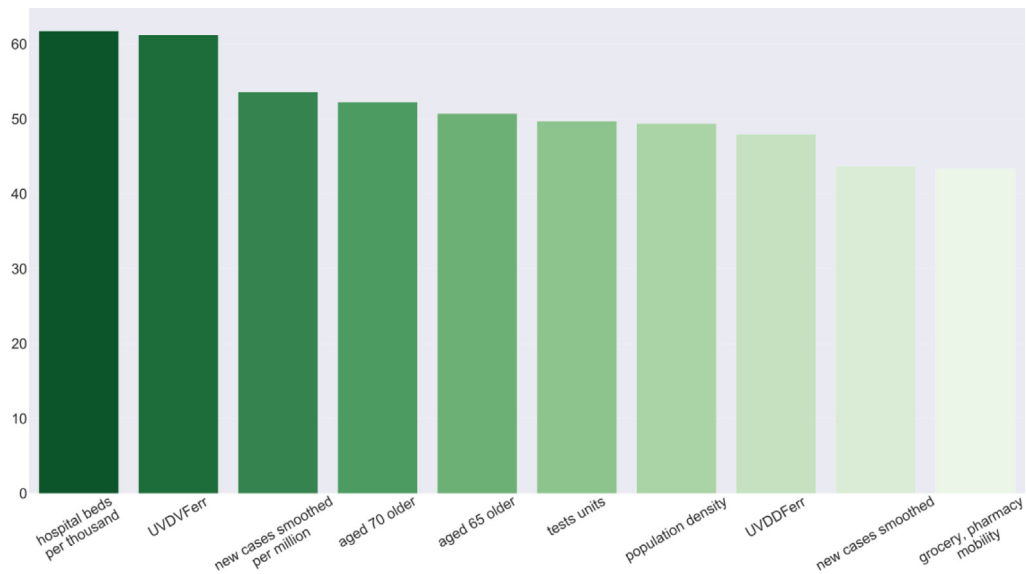
**Fig. 14.** feature attention corresponding to a prediction for new daily COVID-19 cases in Norway.

Fig. 15 shows the rank of contribution band of variables when temporal information is aggregated in case of Norway. It shows that number of hospital bed has highest band revealing that it is dominant feature for daily new cases prediction in Norway. The same dominant feature is highlighted in Italy and Sweden. The network also considers UVDVFerr, new cases smoothed per million, aged 65 and 70 older, number of tests units, population density, UVDDFerr, new cases smoothed and grocery and pharmacy mobility as contributing factors to time-series pattern of daily new cases in Norway. In terms of category, we figure out that the network's attention in Norway is spreading across health facility, environmental, demographic, COVID-19, and mobility features. The mobility feature in Norway is ranked at last out of ten compared to mobility feature in Sweden which is ranked at 4th out of ten, meaning that, people mobility in Sweden

is more contributed to the daily new cases than in Norway (see Fig. 16).

Fig. 16 shows the example of the visual attribution map of Conv-LSTM prediction on a series of daily new COVID-19 cases in Indonesia. Unlike Italy, Sweden, and Norway, which are located in the northern subtropical region, the Conv-LSTM network puts high attention on behavioral factor of the residential percent change from baseline. It regards open spaces are safer than closed spaces like residential, grocery, and pharmacy where human-to-human transmission intensely occurs and open spaces like parks are not given much attention.

Low degree of attention on activity in parks, grocery, and retail and UVIEF indicate that open spaces with low intensity of human-to-human interaction are helped by environmental factors such as UV (UVDDFerr at the beginning of time and UVDVFerr at the end of time). Indonesia's daily new COVID-19 cases also depend



**Fig. 15.** Temporal aggregation of attribution in Italy (x-axis is variables and y-axis is aggregation score).

heavily on the number of tests performed across the country at the beginning of time (number of new tests, total tests per thousand, and tests units). The big population also contributes to the new cases, especially if the number of tests grows over time. The number of hospital's beds for the entire time is also an important factor contributing to new cases smoothed.

In Indonesia, the network shows more attention to the 2-month period between 2020-02-21 and 2020-05-21 as the joint contribution of dominant features, which seems to residential mobility, daily new deaths, number of new tests, total tests per thousand, number of tests units, population, cardiovascular death rate, number of hospital beds per thousand, and UVDDFerr. The number of tests (new tests, total tests per thousand, and the number of tests units) dominates the attention revealing that the daily new cases of COVID-19 in Indonesia depend on its test rate which also relates to its population size. The residential mobility is only behavioral feature that contribute to the daily new cases, meaning that, the open spaces almost has no influence to the prediction of daily new cases of COVID-19.

Fig. 17 shows the rank of the contribution band of variables when temporal information is aggregated in the case of Indonesia. Same with the previously investigated countries, it shows that number of the hospital bed has the highest band. The network also considers new deaths, UVDDFerr, new tests, UVDVFerr, tests units, new cases smoothed per million, aged 70 and 65 older, and total tests per thousand as contributing factors to the time-series pattern of daily new cases. In terms of category, we figure out that the network's attention for Indonesia is spreading across health feature, environmental, demographic, and COVID-19 features with the number of tests related features are dominating with the presence of three features (new tests, tests units, and tests per thousand) among the top ten. There are no mobility features among the top ten revealing that mobility activities have no significant contribution to the dynamics of daily new cases in Indonesia.

## 5. Discussion

While environmental factor correlates to the global spread of COVID-19 pandemic, we believe that it is not just a standalone factor. Some other factors, like morphological and behavioral factors, influence the spread and growth of COVID-19 cases. Human

activity also influences the spread and growth of COVID-19 cases via human-to-human transmission, especially in workplaces, residential, and groceries where direct human interaction is intense in closed spaces. Based on direct evidence, even though there is an indication that COVID-19 is seasonal flu where there is interchanging conditions between northern subtropical, tropical, and southern subtropical locations, some other anticipation should be taken into account:

1. The new normal life is an inevitable thing in daily life where wearing a mask, hand washing, increasing the hospital's capacity, and minimizing the number of activities that make up the crowd should be concerned.
2. Open space is safer than in a closed room with a crowd due to the UV light and air circulation. Unfortunately, the victims mostly occur in closed spaces such as groceries, residential, and workplaces.
3. For tropical countries, an abundance of UV light helps withstand the COVID-19 spread, especially in open space. There must be a good balance between activities inside and outside rooms, especially at noon, where the level UV index is high. In closed spaces like workplaces, it is suggested to expose UV rays in the room before leaving the places when the work hour ends.
4. For subtropical country residents, wearing a mask is compulsory while living in an open space and during the cold season. By the time of the summer season, people in subtropical countries should take advantage of the high UV index level.

## 6. Conclusion

In this work, the multivariate analysis consists of environmental, mobility, demographic, COVID-19, health, health facilities, government, economic, and education categories are considered. The environmental and mobility factors are descriptively analyzed its effect on the dynamics of COVID-19 cases. Moreover, we proposed a model that able to predict the multivariate COVID-19 pandemic data over time named Conv-LSTM. To explain which variables during which period contributing to daily new cases, gradient-based visual attribution is proposed for generating a

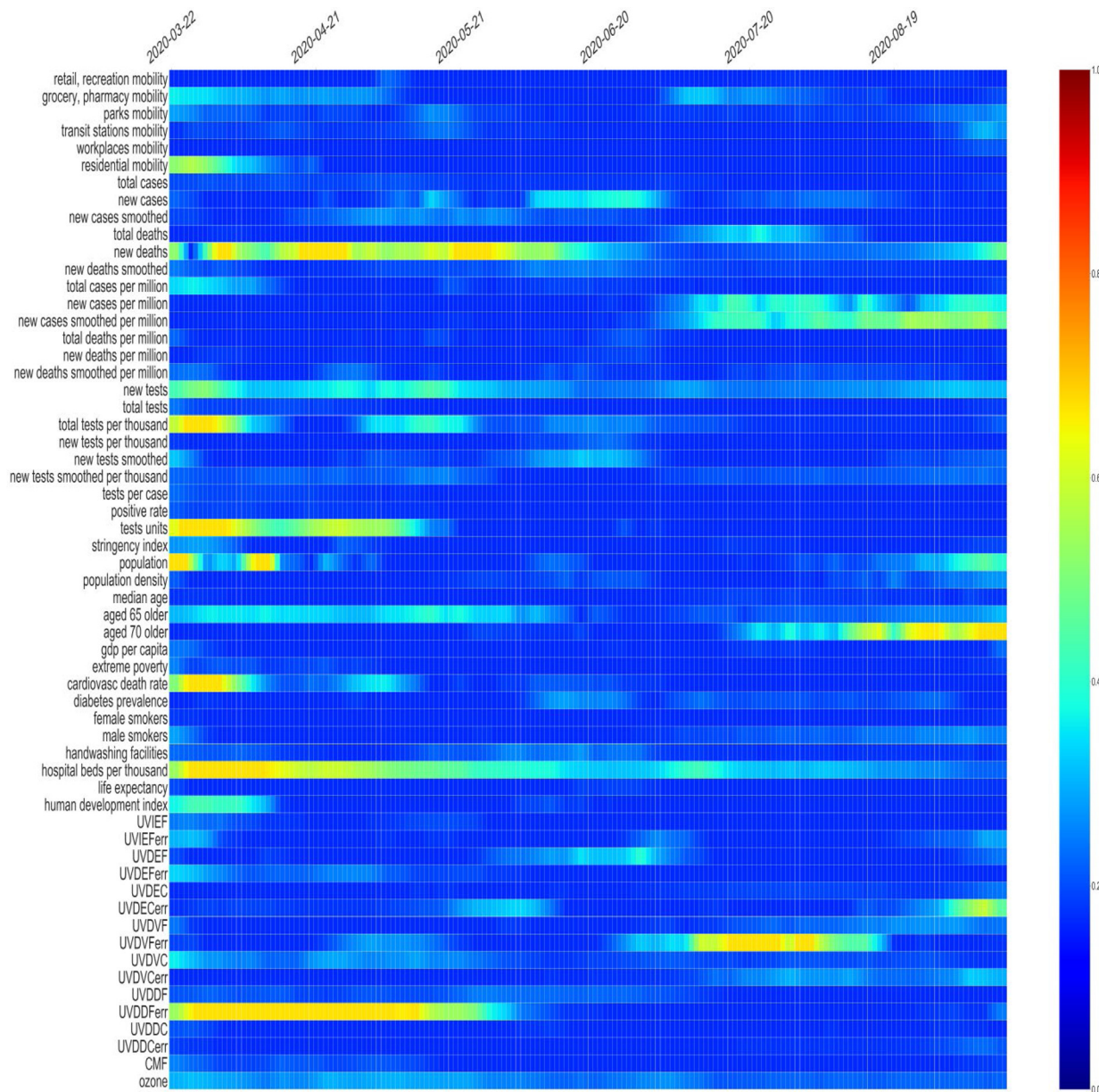


**Fig. 16.** Time and feature attention corresponding to a prediction for new daily COVID-19 cases in Indonesia.

saliency map. Based on results, it is shown that our proposed explainable Conv-LSTM can visualize the spatiotemporal network's attention on multivariate time series data, while not hindering prediction performance. By leveraging the generated saliency map, important factors contributing to the dynamics of COVID-19 pandemics are explained for understanding the current situation about why the number of new cases appears to increase.

For future works, data to be analyzed should be more detailed in terms of the region and the period where the time-series sample is acquired. Moreover, we would consider more data and variables to see more general explanations leveraging the richness of information extracted from big data. There is also the possibility to adapt transformer network to capture important patterns in COVID-19 time-series data. We can implement the proposed method to explain the time-series prediction of other fields such as influenza pandemics, electricity usage, or predictive maintenance. The explanation can be displayed on a web page

or mobile app that shows prediction results and also factors that contribute to those predictions.

#### CRediT authorship contribution statement

**Novanto Yudistira:** Conceptualization, Data curation, Formal analysis, Methodology, Software, Visualization, Writing - original draft. **Sutiman Bambang Sumitro:** Conceptualization, Data curation, Formal analysis, Supervision. **Albert Nahas:** Writing - original draft, Writing - review & editing, Validation. **Nelly Florida Rama:** Data curation, Investigation, Writing - original draft, Writing - review & editing, Validation.

#### Declaration of competing interest

The authors declare that they have no known competing financial interests or personal relationships that could have appeared to influence the work reported in this paper.

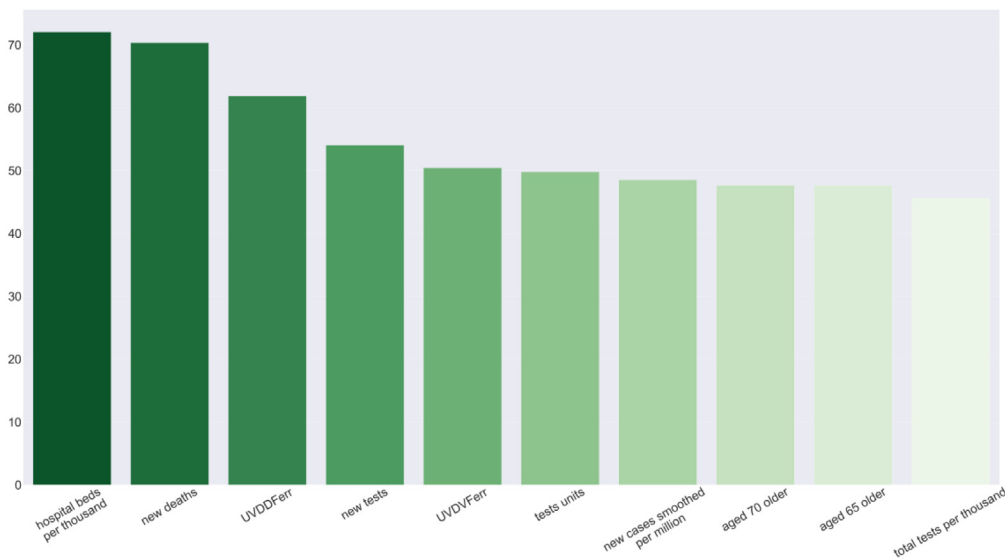


**Fig. 17.** Temporal aggregation of attribution in Indonesia (x-axis is variables and y-axis is aggregation score).

## References

- [1] C. Wang, P.W. Horby, F.G. Hayden, G.F. Gao, A novel coronavirus outbreak of global health concern, *Lancet* 395 (2020) 470–473.
- [2] D. Hui, E.I. Azhar, T.A. Madani, et al., The continuing 2019-ncov epidemic threat of novel coronaviruses to global health—the latest 2019 novel coronavirus outbreak in Wuhan, China, *Int. J. Infect. Dis.* 91 (2020) 264–266.
- [3] N. Singh, M. Kaur, On the airborne aspect of covid-19 corona virus, 2020, arXiv preprint arXiv:2004.10082.
- [4] R. Zhang, Y. Li, A.L. Zhang, Y. Wang, M.J. Molina, Identifying airborne transmission as the dominant route for the spread of covid-19, *Proc. Natl. Acad. Sci.* (2020).
- [5] J.W. Tang, The effect of environmental parameters on the survival of airborne infectious agents, *J. R. Soc. Interface* 6 (2009) S737–S746.
- [6] N. Madhav, B. Oppenheim, M. Gallivan, P. Mulembakani, E. Rubin, N. Wolfe, Pandemics: risks, impacts, and mitigation, in: *Disease Control Priorities: Improving Health and Reducing Poverty*, third ed., The International Bank for Reconstruction and Development/The World Bank, 2017.
- [7] M.M. Jensen, Inactivation of airborne viruses by ultraviolet irradiation, *Appl. Microbiol.* 12 (1964) 418–420.
- [8] K. Bergmann, UU-C irradiation: A new viral inactivation method for biopharmaceuticals, *Am. Pharm. Rev.* (2014) consultado el 01/04/2020.
- [9] J.-L. Sagripanti, C.D. Lytle, Estimated inactivation of coronaviruses by solar radiation with special reference to covid-19, *Photochem. Photobiol.* (2020).
- [10] P. Koronakis, G. Sfantis, A. Paliatsos, J. Kaldellis, J. Garofalakis, I. Koronaki, Interrelations of uv-global/global/di use solar irradiance components and uv-global attenuation on air pollution episode days in athens, Greece, *Atmos. Environ.* 36 (2002) 3173–3181.
- [11] W.F. Barnard, B.N. Wenny, Ultraviolet radiation and its interaction with air pollution, in: *UV Radiation in Global Climate Change*, Springer, 2010, pp. 291–330.
- [12] E. Callaway, D. Cyranoski, S. Mallapaty, E. Stoye, J. Tollefson, The coronavirus pandemic in ve powerful charts, *Nature* 579 (2020) 482–483.
- [13] R. Kuznia, The timetable for a coronavirus vaccine is 18 months. Experts say that's risky, 2020, URL: <https://edition.cnn.com/2020/03/31/us/coronavirus-vaccine-timetable-concerns>.
- [14] T. Koutchma, Advances in ultraviolet light technology for non-thermal processing of liquid foods, *Food Bioprocess Technol.* 2 (2009) 138–155.
- [15] K.N. Prodouz, J.C. Fratantonio, E.J. Boone, R.F. Bonner, Use of laser-uv for inactivation of virus in blood products (1987).
- [16] Amirreza Manteghinejad, Shaghayegh Haghjooy Javanmard, Challenges and opportunities of digital health in a post-COVID19 world, *J. Res. Med. Sci.* 26 (1) (2021) 11.
- [17] Zhengzheng Xing, Jian Pei, Eamonn Keogh, A brief survey on sequence classification, *ACM Sigkdd Explor. Newslett.* 12 (1) (2010) 40–48.
- [18] Muhammad Dur-e Ahmad, Mudassar Imran, Transmission dynamics model of coronavirus COVID-19 for the outbreak in most affected countries of the world, *Int. J. Interact. Multimedia Artif. Intell.* 6 (2) (2020).
- [19] S.J. Fong, G. Li, N. Dey, R.G. Crespo, E. Herrera-Viedma, Finding an accurate early forecasting model from small dataset: A case of 2019-ncov novel coronavirus outbreak, 2020, arXiv preprint arXiv:2003.10776.
- [20] Yann LeCun, Yoshua Bengio, et al., Convolutional networks for images, speech, and time series, *Handb. Brain Theory Neural Netw.* 3361 (10) (1995) 1995.
- [21] Hassan Ismail Fawaz, Germain Forestier, Jonathan Weber, Lhassane Idoumghar, Pierre-Alain Muller, Deep learning for time series classification: a review, 2018, arXiv preprint arXiv:1809.04356.
- [22] Roy Assaf, Anika Schumann, Explainable deep neural networks for multivariate time series predictions, in: *IJCAI*, 2019.
- [23] Anastasia Traskevich, Martin Fontanari, Tourism potentials in post-COVID19: The concept of destination resilience for advanced sustainable management in tourism, *Tour. Plann. Dev.* (2021) 1–25.
- [24] Thomas Hale, Sam Webster, Anna Petherick, Toby Phillips, Beatriz Kira, Oxford COVID-19 Government Response Tracker, Blavatnik School of Government, 2020.
- [25] Google LLC “Google COVID-19 Community Mobility Reports”. <https://www.google.com/covid19/mobility/> Accessed: May-11-2021.
- [26] Felix A. Gers, Jürgen Schmidhuber, Fred Cummins, Learning to forget: Continual prediction with LSTM, (1999) 850–855.
- [27] Shi Xingjian, et al., Convolutional LSTM network: A machine learning approach for precipitation nowcasting, 2015, arXiv preprint arXiv:1506.04214.
- [28] Wenjie Lu, et al., A CNN-LSTM-based model to forecast stock prices, *Complexity* 2020 (2020).
- [29] Zao Zhang, Yuan Dong, Temperature forecasting via convolutional recurrent neural networks based on time-series data, *Complexity* 2020 (2020).
- [30] Ramprasaath R. Selvaraju, Michael Cogswell, Abhishek Das, Ramakrishna Vedantam, Devi Parikh, Dhruv Batra, Grad-cam: Visual explanations from deep networks via gradient-based localization, in: *2017 IEEE International Conference on Computer Vision, ICCV*, IEEE, 2017, pp. 618–626.
- [31] Hannah Ritchie, Esteban Ortiz-Ospina, Diana Beltekian, Edouard Mathieu, Joe Hasell, Bobbie Macdonald, Charlie Giattino, Cameron Appel, Lucas Rodés-Guirao, Max Roser, Coronavirus Pandemic (COVID-19). Published online at OurWorldInData.org. Retrieved from: '['https://ourworldindata.org/coronavirus'](https://ourworldindata.org/coronavirus) (2020) [Online Resource].
- [32] J. Van Geffen, A.R. Van Der, M. Van Weele, M. Allaart, H. Eskes, Surface uv radiation monitoring based on gome and sciamicay, 2004.
- [33] M. Paterlini, ‘Closing borders is ridiculous’: the epidemiologist behind Sweden’s controversial coronavirus strategy, *Nature* (2020).